Propagation of an earthquake triggering front from the 2011 Tohoku-Oki earthquake

Masatoshi Miyazawa[1]

Increases in seismicity have been widely observed at varying distances from the source area following large earthquakes. The increased number of earthquakes are usually called aftershocks if the area is within a rupture length of the mainshock, and called remotely triggered events if they are well beyond that distance. These earthquakes can be explained as being induced by static and/or dynamic stress changes due to the mainshock. However, clear observations of dynamic triggering have been inadequate to differentiate between the two mechanisms. This study shows that early post-seismic events triggered by the 2011 M_w 9.0 Tohoku-Oki earthquake systematically propagated over Japan in a southwestern direction, associated with the strong seismic waves from the source. The propagation front was consistent with the arrivals of large amplitude surface waves traveling at 3.1 to 3.3 km/s and extending to a distance of 1,350 km. There were no observations of triggered earthquakes in the northern direction. Dynamic stress changes toward the north were comparable to or smaller than those necessary for triggering in the southwestern direction. Static stress changes were one to two orders smaller than dynamic stress changes at remote distance, indicating that static stress was not the main mechanism of the triggering. Furthermore, the dynamic stress/strain changes play an important role for remote triggering if the value is more than ∼500 kPa in stress or $\sim 10^{-6}$ in strain.

1. Introduction

Dynamic triggering is known as a process where earthquakes are triggered by transient stress perturbations due to the passage of large seismic waves from an earthquake[*Hill and Prejean*, 2007]. Clear examples include remote triggering at distances of many fault lengths [*Hill et al.*, 1993] and repeated phase triggering from surface waves [*West et al.*, 2005; *Miyazawa and Mori*, 2006; *Wu et al.*, 2011]. Static triggering is based on the idea that permanent stress changes near a source region cause earthquakes via Coulomb stress changes [e.g., *Stein*, 1999]. Quasi-static triggering is also caused by the permanent stress changes but involves some time delay [e.g., *Gomberg*, 1998; *Pollitz and Sacks*, 2002]. In any case, there is an initially stressed state and the change is the triggering stress [*Harris*, 1998]. There have been differing views between the contributions of dynamic and static stress changes in triggering aftershocks [*Felzer and Brodsky*, 2006; *Richards-Dinger et al.*, 2010]. Compared with many observations recognized as static triggering, more observations are required to understand dynamic triggering, because the process fundamentally informs us how an earthquake occurs due to a relatively short-term stress perturbation.

2. Early post-seismicity over Japan

The M_w 9.0 Tohoku-Oki earthquake on March 11, 2011, was followed by many small to large earthquakes over the Japanese Islands [*Hirose et al.*, 2011] (Figure 1). Clarifying the initial distribution of this high rate of seismicity, using the dense seismic network of more than 1,500 seismic stations, makes it possible to investigate how the triggering starts. The Japan Meteorological Agency (JMA) routinely produces a high-quality earthquake catalogue, however the catalogue can miss many small earthquakes immediately after a large mainshock. The missed events are located not only near the source area but over all of Japan, because the large amplitude waves from the mainshock hinders accurate picking of early post-earthquakes. To overcome this difficulty and supplement the JMA earthquake catalogue, I searched for earthquakes with a technique that mainly used a 8–32 hz band-pass filter and other band-pass filters on continuous records from Hi-net borehole stations that had high signal-to-noise ratios. The filtering reduces the seismic waves from the Tohoku-Oki earthquake so that local events can be more easily detected (Figure 2). Identified events close to the stations were located by picking P and S wave arrivals [*Hirata and Matsu'ura*, 1987] using seismograms at the borehole stations and other neighbouring non-borehole stations. I used the velocity model JMA2001, which is the standard model to determine hypocenters in the JMA catalogue. Events observed at only a few stations have larger uncertainties but the location errors are still smaller than or comparable to the symbol size in Figure 1(a). Events could not be detected in northeastern Honshu Island, because of the strong high-frequency waves from the Tohoku-Oki earthquake and its large aftershocks. Also, power failures in the region caused data gaps. The local magnitudes were calculated for the detected earthquakes using the largest amplitude during the S-wave arrivals, however they may be slightly overestimated because of other overlapping waves mainly from the Tohoku-Oki earthquake.

Early post-earthquakes were observed during and after the passage of waves from the Tohoku-Oki earthquake within a distance of 1,350 km, especially in some specific regions, including volcanic areas, areas of previous high seismicity, and plate subduction zones. For example, in the Hida region of central Honshu, which has active volcanoes, a sequence of shallow earthquakes ($M < 5$) was observed, however the seismicity had been rather active even before the Tohoku-Oki earthquake. In the northern Izu islands, increased volcanic earthquakes were observed. It has been reported that volcanic event sequences were induced by the surface waves at Hakone volcano in Honshu [*Yukutake et al.*, 2011], which were not detected in this approach. In contrast to these shallow earthquakes, intra-plate earthquakes at depths of 30 to 40 km within the subducting Philippine Sea plate were also triggered at some distance from

[1]Disaster Prevention Research Institute, Kyoto University, Uji, Kyoto, Japan.

0094-8276/12/$5.00

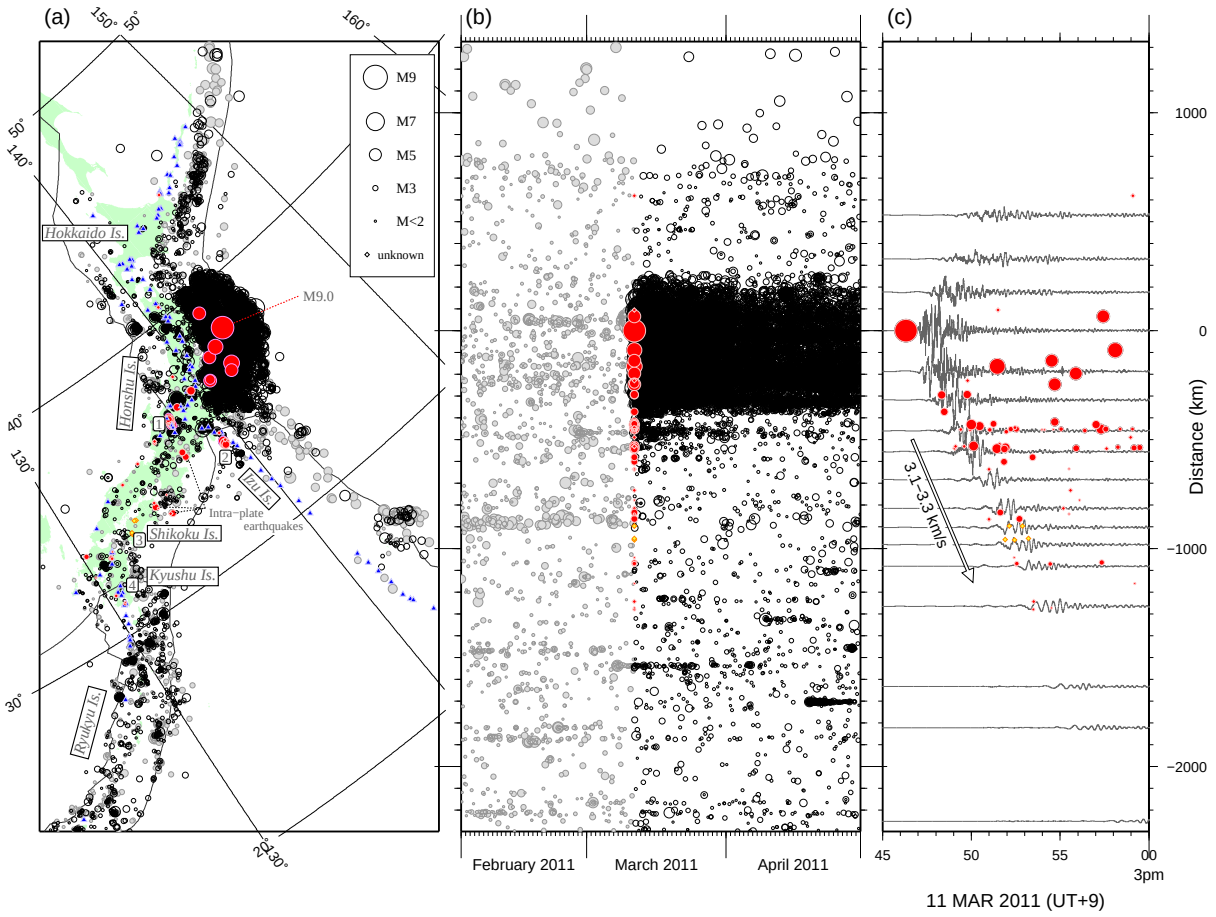

Figure 1. Spatiotemporal distribution of epicenters over Japan before and after the 2011 Tohoku-Oki earthquake (Feb 1, 2011 – Apr 30, 2011). Earthquakes with depths shallower than 100 km are shown. Earthquakes with $M \geq 2$ before and after the 2011 Tohoku-Oki earthquake are indicated by gray and black circles, respectively. The earthquakes with $M < 2$ are shown only for the early post-seismicity. (a) The spatial distribution of epicenters with early post-earthquakes detected in red, and triggered non-volcanic tremor in yellow. Active volcanoes are shown by blue triangles. Regions labeled 1 to 4 are Mt. Hida, northern Izu Is., western Shikoku, and Mt. Kirishima, respectively. Solid lines show plate boundaries [*Bird*, 2003]. (b) The temporal variation of seismicity for distances from the Tohoku-Oki earthquake projected on the vertical axis of map (a). (c) The early post-seismicity together with some vertical components of broadband seismograms at various distances filtered at 0.01 to 1 hz.

the Tohoku region. In western and central Shikoku, triggered non-volcanic tremor was correlated with the large arriving surface waves, as has been previously observed from other earthquakes [*Miyazawa and Mori*, 2006; *Miyazawa and Brodsky*, 2008; *Miyazawa et al.*, 2008]. These early post-earthquakes can be easily identified as triggered events from the abrupt increased seismicity after the Tohoku-Oki earthquake (Figure 1(c) and Figure S1 in the auxiliary material). The early post-seismicity has a different spatial pattern compared to the later post-seismicity that occurred across Japan over the next days to weeks (Figure S2 in the auxiliary material). The later activity was probably caused by static stress changes [*Toda et al.*, 2011; *Ishibe et al.*, 2011; *Okada et al.*, 2011]. There is a delay in the activation at the locations of the static triggering process, however, the delay does not have any clear patterns and is not yet understood. The increases in seismicity of moderate ($M5$ to 6) earthquakes were found only within about 3 rupture lengths of the mainshock, which is consistent with the results for triggered activity from moderate earthquakes [*Parsons and Velasco*, 2011]. Also no triggering of earthquakes was found beyond 1,400 km southwest of the epicenter, although detection is not as good because there are fewer seismic stations at the farther distances which are mainly offshore. Mt. Kirishima on Kyushu Island, at a distance of about 1,300 km, has had active eruptions since January 2011, however there was no observed change in the volcanic and seismic activity.

As can be seen in Figure 1, the triggered earthquakes during the first 14 minutes progressively occurred toward the southwest as a function of time. I estimated the propagation velocity using a slant stack type of analysis. For assumed values of the propagation velocity, the cumulative number of earthquakes is counted that fall within a moving time window determined by the propagation velocity. The seismicity rate is defined as the cumulative number of earthquakes within a designated time window, normalized by the maximum value. In order to avoid apparent high rates due to the earthquake clustering at a specific distance, the rate is weighted for values where events were broadly distributed over distance. The velocity that has the highest rate is determined to be the propagation velocity and its intercept gives the time when the front starts at the source. Using a 150 s time window, which was the duration of the mainshock

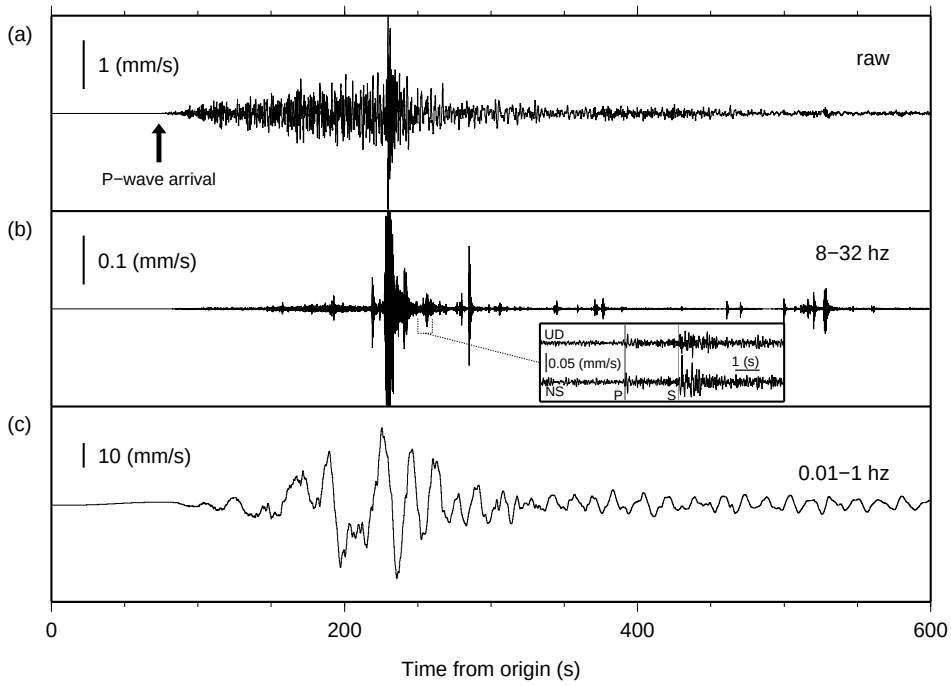

Figure 2. Example of waveforms in the Mt. Hida volcanic region, (labeled "1" in Figure 1(a)). (a) The unfiltered vertical component recorded by 1 hz seismometer at the borehole station KTRH. (b) The waveform filtered with a pass-band of 8 to 32 hz, which shows local triggered events. The inset shows an example of a triggered event on UD and NS components and its P and S wave arrivals. (c) The waveform filtered with a pass-band of 0.01 to 1 hz after removing the instrument response.

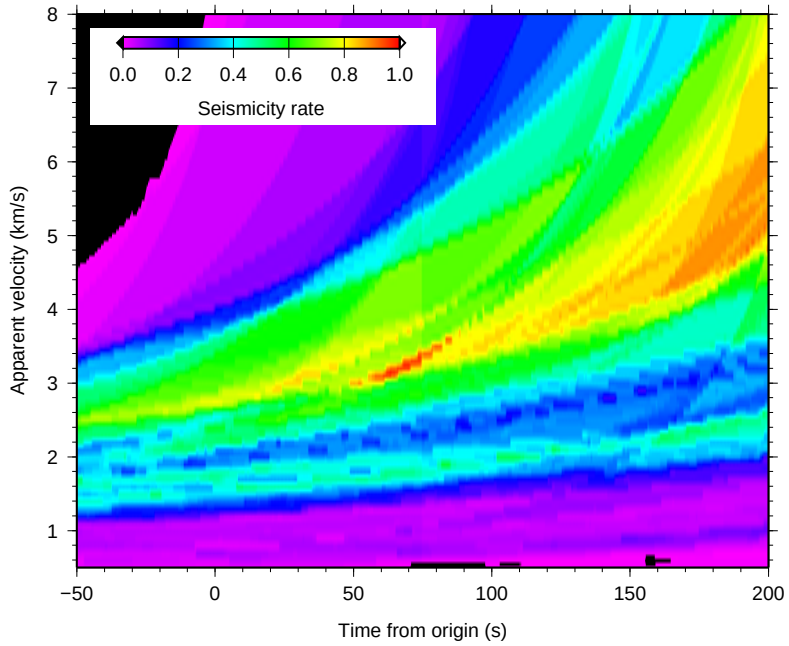

Figure 3. Seismicity rate for assumed propagation velocities as a function of time from the mainshock. The seismicity rate was defined as the cumulative number of earthquakes within a designated time window of 150 s, normalized by the maximum value. In order to avoid apparent high rates due to the earthquake clustering at a specific distance, the rate was weighted for values where events were broadly distributed over distance. The highest value was found at times of 61 to 74 s for velocities of 3.1 to 3.3 km/s.

rupture, this procedure gave a propagation velocity of 3.1 to 3.3 km/s (Figure 3). The intercept of 61 to 74 s was consistent with the observations that the largest amplitude waves from the source were generated about 60 to 80 s after the

initiation [*Ide et al.*, 2011; *Shao et al.*, 2011; *Suzuki et al.*, 2011]. This shows the clear propagation speed of triggered early post-earthquakes.

3. Discussion

Dynamic stress changes from both Love and Rayleigh waves have the potential for earthquake triggering [*Hill*, 2010]. The propagation speed found in this study seems consistent with the Rayleigh wave velocity for periods of 10–20 s, which cause large normal stress changes in the crust [*Miyazawa and Brodsky*, 2008]. However, due to the heterogeneity of the complicated subduction zone structure along the Japanese Islands, no specific phase of the surface waves can be identified as the triggering wave. Static stress changes associated with the near-field term also propagate at 3–4 km/s [*Wideman and Major*, 1967; *Okubo et al.*, 2004; *Kinoshita and Takagishi*, 2011], so it is difficult to distinguish between static and dynamic triggering using the propagation velocity. During the passage of seismic waves, the sum of the dynamic stress amplitude together with the ramp-function of the near-field term is larger than just the static change at any distance. Usually the dynamic stress changes from the surface wave decreases proportional to the distance, while static stress changes decrease as the 3rd power of distance (Figure 4). The farther the distance, the more effective dynamic stress is for triggering than static stress. Since the triggering stress depends on the source mechanism of triggered events, which is unclear in this case, I simply calculated the maximum dynamic and static stress values at a depth of 10 km. For the dynamic stress changes, three component broad-band seismograms at 71 broadband seismic stations were used to obtain spatial derivatives of displacements via transport kernels, and from the spatial derivatives the dynamic strain and stress tensors can be calculated [*Miyazawa and Brodsky*, 2008]. The static stress changes were calculated using the source model derived from GPS observations, which is available from the Geospatial Information Authority of Japan (http://www.gsi.go.jp/), and assuming a half-space [*Okada*, 1992]. The Lame's parameters were assumed to be $\lambda = \mu = 30$ GPa. The maximum magnitude of eigenvalues of the dynamic/static stress tensor was given as the representative maximum stress load at each position. The static stress changes in the Hida and northern Izu regions at distance of around 500 to 540 km were on the order of 100 kPa, which is comparable with or almost one order smaller than the dynamic stress changes, while beyond 1,000 km the static stress is about two orders smaller than the dynamic stress. In many regions of triggered events found in the propagation front, the dynamic stress overwhelms the static stress change.

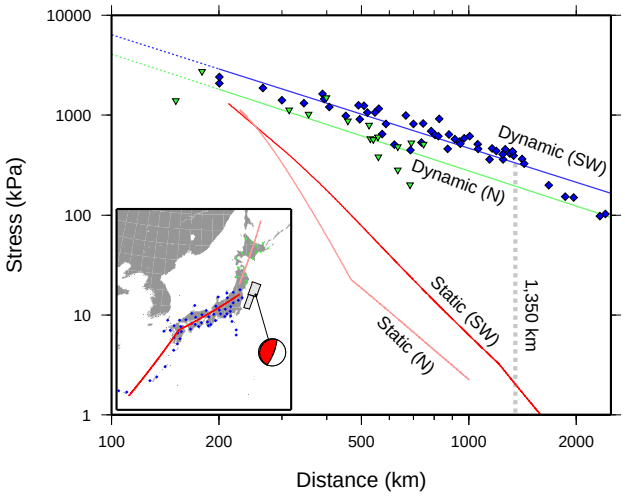

Figure 4. Static and dynamic stress changes at a depth of 10 km as a function of distance from the 2011 Tohoku-Oki earthquake for directions toward the southwest (SW) and north (N). The maximum magnitudes of the eigenvalues of the stress tensor at a depth of 10 km at each distance are plotted by red lines for static stress changes and by blue (southwest direction) and green (north direction) symbols for the dynamic stress changes. Static stress changes are calculated using the geodetic source model (see the text), and the dynamic stress changes are obtained at 71 broadband seismic stations with the lines showing a linear regression fit as a function of distance. The inset map shows the profile lines along which the static stress changes were calculated and the locations of the broadband stations where the dynamic stress changes were calculated. Also shown are the CMT solution (www.globalcmt.org) and the rectangular fault model of the mainshock used to calculate the static stress change.

A propagation of triggered events toward the northeast was not found within the seismic network in northern Japan, where the dynamic and static stress changes were, respectively, 1.4 to 1.7 times and about 3 times smaller than those toward the southwest (Figure 4), due to the directivity of the rupture propagation toward the west and southwest [*Ide et al.*, 2011]. Note that the seismic network is about the same density in northern Japan so it should be able to detect small triggered events. Seismicity changes during the following months were small as well [*Hirose et al.*, 2011]. At the far edge of the observed triggering propagation front in the southwestern direction (distance of 1,350 km), the dynamic and static stress changes were ∼500 kPa and ∼2 kPa, respectively. In central Hokkaido at distance of ∼500 km, the dynamic stress change was also ∼500 kPa, but the static stress change was about 20 kPa. There were no observed triggered events in this region that had relatively large value of static stress change with small dynamic stress perturbations. This suggests that the static stress changes were not the primary triggering mechanisms of the early post-seismicity. Also, dynamic stress changes exceeding a threshold value seem to be a necessary but not sufficient condition for triggering. The value of ∼500 kPa corresponds to a strain of $\sim 3 \times 10^{-6}$, which is consistent with the earthquake dynamic triggering threshold inferred experimentally [*Johnson and Jia*, 2005].

The directivity of the mainshock propagating in the west and southwest directions produced larger seismic waves toward the southwest, which then resulted in the early post-earthquake triggering toward the southwest but not toward the north. Similar patterns of triggering related to the rupture directivity have been observed for remotely triggered earthquakes of the 1992 Landers, the 1999 Hector Mine, and the 2004 Denali earthquakes [*Eberhart-Phillips et al.*, 2003; *Gomberg et al.*, 2001, 2004].

4. Conclusions

From the observations of the systematic propagation of triggered events over Japan at the surface wave velocity and the difference of the triggering pattern in different directions, I conclude that the early post-seismicity was triggered by the dynamic stress changes from the 2011 Tohoku-Oki earthquake. The static stress changes were one to two orders smaller than the dynamic stress changes at remote distances up to 1,400 km. The triggering propagation seems to

indicate a threshold level of ∼500 kPa, or strain on the order of 10^{-6}, is necessary for direct triggering of earthquakes at these locations. Also, the later post-earthquakes, which are inferred to have been triggered largely by static stresses, are not spatially correlated with the early post-earthquakes.

Acknowledgments. Discussion with Jim Mori and Shinji Toda helped develop this study. I thank Ruth Harris, Chunquan Wu, and an anonymous reviewer for careful and thoughtful reviews. This study was partially supported by the Ministry of Education, Culture, Sports, Science and Technology (MEXT) of Japan, under its Observation and Research Program for Prediction of Earthquakes and Volcanic Eruptions. Figures were drawn using the Generic Mapping Tools [*Wessel and Smith*, 1998]. I used the JMA earthquake catalogue.

References

Bird, P. (2003), An updated digital model of plate boundaries, *Geochem. Geophys. Geosyst.*, *4*(3), 1027, doi:10.1029/2001GC000252.

Eberhart-Phillips, D. et al. (2003), The 2002 Denali fault earthquake, Alaska: A large magnitude, slip-partitioned event, *Science*, *300*, 1113–1118, doi:10.1126/science.1082703.

Felzer, K. R., and E. E. Brodsky (2006), Decay of aftershock density with distance indicates triggering by dynamic stress, *Nature*, *441*, 735–738, doi:10.1038/nature04799.

Gomberg, J., N. M. Beeler, M. L. Blanpied, and P. Bodin (1998), Earthquake triggering by transient and static deformations, *J. Geophys. Res.*, *103*(B10), 24,411–24,426, doi:10.1029/98JB01125.

Gomberg, J., P. Bodin, K. Larson, and H. Dragert (2004), Earthquake nucleation by transient deformations caused by the M = 7.9 Denali, Alaska, earthquake, *Nature*, *427*, 621–624, doi:10.1038/nature02335.

Gomberg, J., P. A. Reasenberg, P. Bodin, and R. A. Harris (2001), Earthquake triggering by seismic waves following the Landers and Hector Mine earthquakes, *Nature*, *411*, 462–466, doi:10.1038/35078053.

Harris, R. A. (1998), Introduction to special section: Stress triggers, stress shadows, and implications for seismic hazard, *J. Geophys. Res.*, *103*(B10), 24,347–24,358, doi:10.1029/98JB01576.

Hill, D. P. (2010), Surface-wave potential for triggering tectonic (nonvolcanic) tremor, *Bull. Seismol. Soc. Am.*, *100*, 1859–1878, 10.1785/0120090362.

Hill, D. P., and S. G. Prejean (2007), Dynamic triggering, in *Treatise on Geophysics; Earthquake Seismology*, edited by H. Kanamori, pp. 257–291, Elsevier B.V., Amsterdam.

Hill, D. P. et al. (1993), Seismicity remotely triggered by the magnitude 7.3 Landers, California, earthquake, *Science*, *260*, 1617–1623, 10.1126/science.260.5114.1617.

Hirata, N., and M. Matsu'ura (1987), Maximum-likelihood estimation of hypocenter with origin time eliminated using nonlinear inversion technique, *Phys. Earth Plant. Inter.*, *47*, 50–61.

Hirose, F., K. Miyaoka, N. Hayashimoto, T. Yamazaki, and M. Nakamura (2011), Outline of the 2011 off the Pacific coast of Tohoku Earthquake (Mw 9.0) –Seismicity: foreshocks, mainshock, aftershocks, and induced activity–, *Earth Planets and Space*, *63*, 513–518, doi:10.5047/eps.2011.05.019.

Ide, S., A. Baltay, and G. C. Beroza (2011), Shallow Dynamic Overshoot and Energetic Deep Rupture in the 2011 Mw 9.0 Tohoku-Oki Earthquake, *Science*, *332*, 1426–1429, doi:10.1126/science.1207020.

Ishibe, T., K. Shimazaki, K. Satake, and H. Tsuruoka (2011), Change in seismicity beneath the Tokyo metropolitan area due to the 2011 off the Pacific coast of Tohoku Earthquake, *Earth Planets and Space*, *63*, 731–735, doi:10.5047/eps.2011.06.001.

Johnson, P. A., and X. Jia (2005), Nonlinear dynamics, granular media and dynamic earthquake triggering, *Nature*, *437*, 871–874, doi:10.1038/nature04015.

Kinoshita, S., and M. Takagishi (2011), Generation and propagation of static displacement estimated using KiK-net recordings, *Earth Planets and Space*, *63*, 779–783, doi:10.5047/eps.2011.05.003.

Miyazawa, M., and E. E. Brodsky (2008), Deep low-frequency tremor that correlates with passing surface waves, *J. Geophys. Res.*, *113*, B01307, doi:10.1029/2006JB004890.

Miyazawa, M., E. E. Brodsky, and J. Mori (2008), Learning from dynamic triggering of low-frequency tremor in subduction zones, *Earth Planets Space*, *60*, e17–e20.

Miyazawa, M., and J. Mori (2006), Evidence suggesting fluid flow beneath Japan due to periodic seismic triggering from the 2004 Sumatra-Andaman earthquake, *Geophys. Res. Lett.*, *33*, L05303, doi:10.1029/2005GL025087.

Okada, T. et al. (2011), Shallow inland earthquakes in NE Japan possibly triggered by the 2011 off the Pacific coast of Tohoku Earthquake, *Earth Planets and Space*, *63*, 749–754, doi:10.5047/eps.2011.06.027.

Okada, Y. (1992), Internal deformation due to shear and tensile faults in a half-space, *Bull. Seismol. Soc. Am.*, *82*, 1018–1040.

Okubo, M., Y. Asai, H. Aoki, and H. Ishii (2004), The seismological and geodetical roles of strain seismogram suggested from the 2004 off the Kii peninsula earthquakes, *Earth Planets and Space*, 57, 303–308.

Parsons, T., and A. A. Velasco (2011), Absence of remotely triggered large earthquakes beyond the mainshock region, *Nature Geoscience*, *4*, 321–316, doi:10.1038/ngeo1110.

Pollitz, F. F., and I. S. Sacks (2002), Stress Triggering of the 1999 Hector Mine Earthquake by Transient Deformation Following the 1992 Landers Earthquake, *Bull. Seismol. Soc. Am.*, *92*, 1487-1496, doi:10.1785/0120000918.

Richards-Dinger, K., R. S. Stein, and S. Toda (2010), Decay of aftershock density with distance does not indicate triggering by dynamic stress, *Nature*, *467*, 583–586, doi:10.1038/nature09402.

Shao, G., X. Li, C. Ji, and T. Maeda (2011), Focal mechanism and slip history of the 2011 Mw 9.1 off the Pacific coast of Tohoku Earthquake, constrained with teleseismic body and surface waves, *Earth Planets and Space*, *63*, 559–564, doi:10.5047/eps.2011.06.028.

Stein, R. S. (1999), The role of stress transfer in earthquake occurrence, *Nature*, *401*, 605–609.

Suzuki, W., S. Aoi, H. Sekiguchi, and T. Kunugi (2011), Rupture process of the 2011 Tohoku-Oki mega-thrust earthquake (M9.0) inverted from strong-motion data, *Geophys. Res. Lett.*, *38*, L00G16, doi:10.1029/2011GL049136.

Toda, S., J. Lin, and R. S. Stein (2011), Using the 2011 Mw 9.0 off the Pacific coast of Tohoku Earthquake to test the Coulomb stress triggering hypothesis and to calculate faults brought closer to failure, *Earth Planets and Space*, *63*, 725–730, doi:10.5047/eps.2011.05.010.

Wessel, P., and W. H. F. Smith (1998), New, improved version of generic mapping tools released, *Eos Trans. AGU*, *79*(47), 579, doi:10.1029/98EO00426.

West, M., J. J. Sánchez, and S. R. McNutt (2005), Periodically triggered seismicity at Mount Wrangell, Alaska, after the Sumatra earthquake, *Science*, *308*, 1144–1146, doi:10.1126/science.1112462.

Wideman, C. J., and M. W. Major (1967), Strain steps associated with earthquakes, *Bull. Seismol. Soc. Am.*, *57*, 1429–1444.

Wu, C., Z. Peng, W. Wang, and Q.-F. Chen (2011), Dynamic triggering of shallow earthquakes near Beijing, China, *Geophys. J. Int.*, *185*, 1321–1334, doi:10.1111/j.1365-246X.2011.05002.x.

Yukutake, Y., R. Honda, M. Harada, T. Aketagawa, H. Ito, and A. Yoshida (2011), Remotely-triggered seismicity in the Hakone volcano following the 2011 off the Pacific coast of Tohoku Earthquake, *Earth Planets and Space*, *63*, 737–740, doi:10.5047/eps.2011.05.004.

Masatoshi Miyazawa, Disaster Prevention Research Institute, Kyoto University, Uji, Kyoto 611-0011, Japan. (miyazawa@rcep.dpri.kyoto-u.ac.jp)

Appendix A: Auxiliary Material for Paper 2011GL049795

Propagation of an earthquake triggering front from the 2011 Tohoku-Oki earthquake

Masatoshi Miyazawa
Disaster Prevention Research Institute, Kyoto University, Uji, Japan

Miyazawa, M. (2011), Propagation of an earthquake triggering front from the 2011 Tohoku-Oki earthquake, Geophys. Res. Lett., 38, L23307, doi:1029/2011GL049795.

A1. Introduction:

The auxiliary material contains two figures showing the background seismicity and the early post-seismicity as well as the seismicity change estimated by the beta-value.

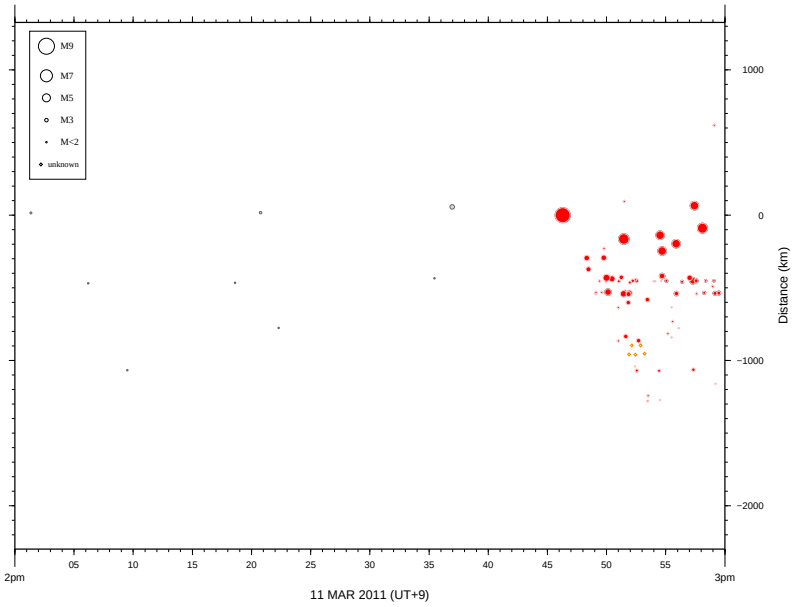

Figure S1. The background seismicity and the early post-seismicity. Labels are the same as those in Figure 1.

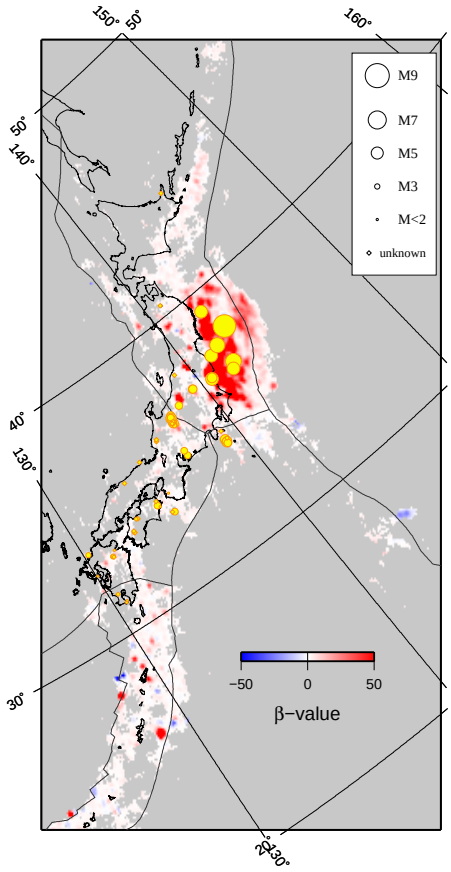

Figure S2. The seismicity change estimated by the beta-value. The rate changes were calculated for 100 days after the Tohoku-Oki earthquake with respect to the background period one year before. Events with magnitude larger than 2 and depth shallower than 100 km were used from the JMA catalogue. Early post-seismic events are indicated by yellow symbols.